Benefits of Operating Doubly Fed Induction Generators by Modular Multilevel Matrix Converters

Felix Kammerer, Mario Gommeringer, Johannes Kolb, Michael Braun
Institute of Electrical Engineering (ETI) - Electrical Drives and Power Electronics
Karlsruhe Institute of Technology (KIT), Kaiserstr. 12, 76131 Karlsruhe, Germany
Tel.: +49 721 608 42461, E-mail: felix.kammerer@kit.edu

Abstract

The benefits of supplying the rotor circuit of a Doubly Fed Induction Generator (DFIG) by the Modular Multilevel Matrix Converter (M3C) are presented. The M3C allows higher rotor voltages, lower rotor currents and a higher redundancy compared to existing solutions. Filters are dispensable due to the generated multilevel voltages. In case of a line voltage drop the M3C arm voltages can be used to generate temporarily higher rotor voltages which may help to control the rotor currents during faults.

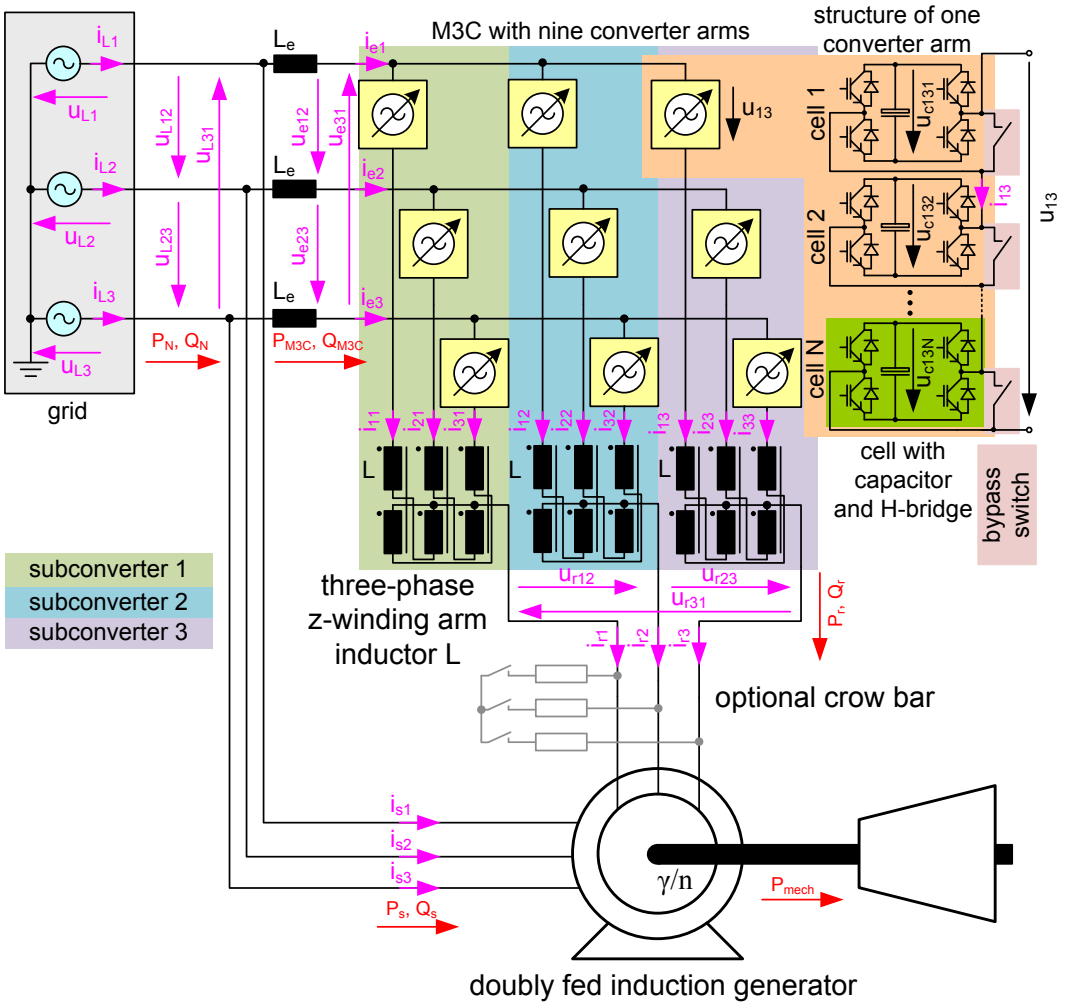

Figure 1: Modular Multilevel Matrix Converter (M3C) for feeding the rotor circuit of a Doubly Fed Induction Generator (DFIG)

1 Introduction

Fig. 1 shows the Modular Multilevel Matrix Converter (M3C) for feeding the rotor circuit of a Doubly Fed Induction Generator (DFIG). The stator of the DFIG is directly connected to the grid. The M3C converts the frequency between the grid and the rotor circuit and allows to control the rotor currents i_{rx}, $x \in \{1, 2, 3\}$. By controlling the rotor currents i_{rx} it is possible to adjust the speed and reactive power or the active and reactive power of the DFIG independently. This can be realized by a stator flux oriented vector control [1].

The M3C (fig. 1) consists of 3 identical subconverters which are directly connected to the grid via the optional line inductors L_e or if necessary with a standard transformer. Each subconverter connects the three input phases via three converter arms and their corresponding arm inductors or the coupled z-winding arm inductor L to one rotor phase. The converter arms are assembled as N series-connected cells which include a H-bridge and a DC-capacitor. A detailed description of the M3C can be found in the following publications: [2] presents the investigation of the suitability of the M3C for high power low speed drives applications. In [3] a cascaded vector control scheme together with the coupled z-winding arm inductor L is presented and extended in [4]. [5] gives a method to estimate the required amount of capacitance installed in the M3C and a detailed description of the coupled z-winding arm inductor L. In [6] an alternative control scheme and a method to reduce the energy pulsation in the converter arms at very low output frequencies are presented. This method uses a phase modulation of the internal currents instead of the amplitude modulation which was proposed in [2] to avoid singularities and therefore very high energy pulsations at several output frequencies.

1.1 Power balance of the Doubly Fed Induction Generator

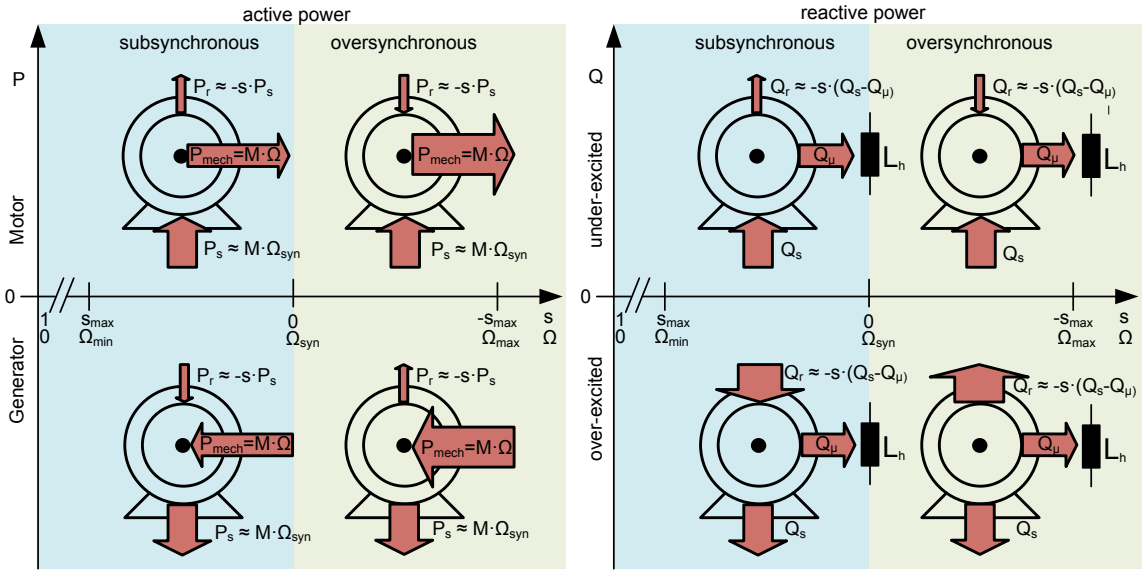

Figure 2: Active and reactive power balance of the DFIG depending on the operation point

Fig. 2 shows the power balance of the DFIG. The active rotor power P_r depends on the slip $s = \frac{\omega_r}{\omega_s}$ and therefore from the required speed range and the stator active power P_s:

$$P_r \approx -s \cdot P_s \tag{1}$$

Neglecting losses, the active stator power P_s corresponds to the mechanical power at the synchronous operation point, depending on the torque M and the synchronous speed Ω_{syn}:

$$P_s \approx M \cdot \Omega_{syn} \tag{2}$$

The mechanical power P_{mech} is the sum of the rotor and stator active power:

$$P_{mech} \approx P_r + P_s = (1 - s) \cdot M \cdot \Omega_{syn} \tag{3}$$

The reactive rotor power Q_r depends also on the speed range of the DFIG and the required stator reactive power Q_s, with an offset from the magnetizing reactive power $Q_\mu > 0$:

$$Q_r \approx -s \cdot (Q_s - Q_\mu) \tag{4}$$

Using (1) and (4), the apparent rotor power S_r which must be delivered by the M3C can be calculated to:

$$S_r \approx \sqrt{(-s \cdot P_s)^2 + (-s \cdot (Q_s - Q_\mu))^2} \tag{5}$$

(5) shows that the maximum apparent rotor power $S_{r,max}$ for the dimensioning of the M3C depends on the maximum slip $|s_{max}|$ and the maximum active P_s and reactive power Q_s which must be delivered to the grid. The required rotor voltages $|\underline{U}_{rx}|$ and rotor currents $\underline{I}_{rx}$ for the dimensioning of the M3C depend on the voltage transformation ratio of the DFIG $k_{DFIG} = \frac{|\underline{U}_{rx}|}{|\underline{U}_{Lx}|}$, neglecting the stator and rotor resistance R_s and R_r and the stator and rotor stray inductance $L_{s\sigma}$ and $L_{r\sigma}$ due to their low values:

$$|\underline{U}_{rx}| \approx |s| \cdot k_{DFIG} \cdot |\underline{U}_{Lx}| \tag{6}$$

$$\underline{I}_{rx} \approx -\frac{1}{k_{DFIG}} \cdot (\underline{I}_{sx} - \underline{I}_\mu) \tag{7}$$

(7) shows that the rotor currents $\underline{I}_{rx}$ are proportional to the stator currents $\underline{I}_{sx}$ with an offset of the magnetization current $\underline{I}_\mu$ at the whole speed range. This means, that limiting the rotor currents $\underline{I}_{rx}$ also limits the stator active and reactive power P_s and Q_s and therefore the mechanical power P_{mech} and the torque M. According to (6) the highest rotor voltage $|\underline{U}_{rx,max}|$ occurs at the maximum slip $|s_{max}|$.

2 Benefits of supplying the rotor circuit by the Modular Multilevel Matrix Converter

2.1 General benefits of the Doubly Fed Induction Generator

Considering (1) - (7), the DFIG together with the M3C allows to construct very big variable speed generator units with a limited speed range. Only the rotor power P_r has to be transfered via slip rings and the converter to the grid. This reduces the converter size and losses compared to full power converter solutions. Therefore the DFIG is suitable for wind power applications and pumped storage plants [7, 8]. The efficiency of the connected turbine increases especially under part load conditions due to the variation of speed. This is reported for pumped storage plants [7, 8] and can be expected also for thermal power plants in the future which have to compensate fluctuating generation from renewable energy sources. Another degree of freedom is the dynamic decoupling of the grid power P_N from the mechanical power P_{mech}. Therefore the freewheeling effect can be used to stabilize the grid much faster than using a synchronous machine [7]. Additionally, torque peaks from the turbine can be separated from the grid to avoid disturbances in the electric system.

2.2 Scalability of the M3C

One of the major benefits of the M3C is the scalability in the voltage range. This is possible due to the fact, that the M3C converter arms (Fig. 1) are assembled as N series-connected cells. Each cell consists of a DC-capacitor and a H-bridge with the corresponding cell electronics. The semiconductor switches only have to block the individual cell capacitor voltages u_{cxyz} ($x, y \in \{1, 2, 3\}$: number of the connected input and output phase, $z \in \{1, 2, ..., N\}$: number of the cell). This allows to use conventional low voltage switches to construct medium voltage converters. To achieve higher rotor voltages $|\underline{U}_{rx}|$, a higher arm capacitor voltage u_{cxy} is necessary. This can be realized by using a higher number of cells per arm N. Therefore the M3C is not limited by semiconductor blocking voltages like cycloconverters or back-to-back voltage source converters which are used today to feed DFIGs in the high power range [7, 8, 9]. The required minimum arm capacitor voltage $u_{cxy,min}$ is the sum of the minimum cell capacitor voltages $u_{cxyz,min}$ in one converter arm and can be calculated to [3]:

$$u_{cxy,min} = \sum_{z=1}^{N} u_{cxyz,min} = N \cdot u_{cxyz,min} \geq \hat{u}_{ex} + \hat{u}_{rx}. \tag{8}$$

To achieve the lowest possible energy pulsation ΔW_{arm} in the converter arms the voltage transfer ratio of the M3C $k_{M3C} = \frac{|\underline{U}_{rx}|}{|\underline{U}_{ex}|}$ has to be selected to $k_{M3C} = 1$, this results in $|\underline{U}_{rx,max}| = |\underline{U}_{ex,max}|$. This reduces the required arm capacitance C_{arm} which must be installed in the M3C [5].

For a better use of the scalability, higher rotor voltages $|\underline{U}_{rx}|$ compared to state of the art solutions are possible. This allows a higher voltage transformation ratio k_{DFIG} of the DFIG and results in significantly lower rotor currents (7) which must be transferred via slip rings to the rotor, however the winding isolation has to be designed for the higher rotor voltages $|\underline{U}_{rx}|$.

The arm currents i_{xy} contain input i_{ex}, rotor i_{rx} and internal i_i current components (see [3, 4, 5]). The commutation loops of the M3C are inside of the cells and the arm currents are flowing continuously in the converter arms. So no special low inductive connections between the cells are necessary. This results in a much easier design of the M3C compared to MW voltage source converters which requires a low inductive DC-bus with a length of several ten meters.

The M3C is also scalable in the current range, using parallelization of cells or semiconductors. Another possibility is the parallelization of the whole M3C or complete converter arms, here additional (coupled) inductors are necessary to decouple the units.

2.3 Redundancy of the M3C

The second benefit is the scalability of the desired redundancy in case of component failures. Due to its modular structure the M3C remains operating with failed cells in the converter arms. For this, additional bypass switches (see fig. 1) must be installed and closed in case of a failure to bypass the failed cells. The bypass switch consists of a mechanical switch or two anti-parallel thyristors. According to the customer requirements two principal redundancy strategies are possible:

- Installation of additional redundancy cells to remain operating with full power after cell failures.
- Reduction of the maximum rotor voltage $|\underline{U}_{rx,max}|$ according to the number of failed cells per arm.

In the first case, to remain operating with full power after F-cell failures per arm the following oversizing for redundancy R of the M3C is necessary ($k_{M3C} = 1$):

$$R_{N-F}(\%) = \frac{F}{N} \cdot 100\% \qquad F = \text{Number of failed cells per arm} \tag{9}$$

For a M3C with $N = 10$ cells per arm and an $(N-1)$-redundancy a oversizing of 10% is needed (9), so one additional redundancy cell per arm has to be installed. More redundant cells per arm can be installed, depending on the application requirements. In comparison the cycloconverter in the pump-storage plant Goldisthal (Germany) needs a 50% oversizing of the converter to remain operating at full power after a single componement failure $(N-1)$ [7, 8].

Conversely, if no extra cells for redundancy are installed, the maximum rotor voltage $|\underline{U}_{rx,max}|$ is reduced according to the number of failed cells ($k_{M3C} = 1$):

$$|\underline{U}_{rx,max,N-F}| = \frac{N-2F}{N} \cdot |\underline{U}_{rx,max}| \tag{10}$$

According to (6) the maximum slip and therefore the maximum rotor power P_r (1) is reduced:

$$|s_{max,N-F}| = \frac{N-2F}{N} \cdot |s_{max}| \tag{11}$$

Fig. 3 shows the reduction of the reachable speed range, depending of the number of failed cells F for $N = 10$. For one failed cell per arm, the speed range will be only reduced by about 20% without reduction of the rotor currents i_{rx}. Therefore the stator currents i_{sx}, the stator power P_s (2) and the torque M are not reduced like in case of the cycloconverter with a failed parallel bridge [7, 8]. Furthermore, the operation of the DFIG as conventional synchronous machine is possible until 50% of the cells per arm are failed.

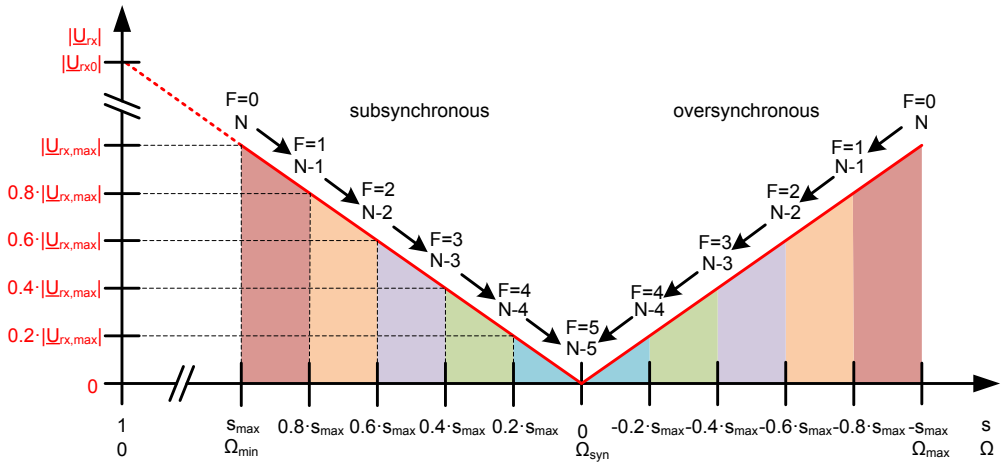

Figure 3: Reduction of the usable speed range of the DFIG depending on the number of failed cells per arm F for a M3C with $N = 10$ cells per arm

2.4 Rotor and line voltage quality of the M3C

A third benefit of the M3C is the multilevel waveform of the generated voltages, which is very close to the sinusoidal fundamental waveform with few harmonics on the line side u_{ex} and on the

rotor side u_{rx}. This is very important for the DFIG, due to the fact that rotor current harmonics ν_{ir} ($\nu \in \{1, 2, 3, ...\}$: number of harmonics) cause subharmonics in the stator currents i_{sx} with the angular frequencies $\omega_{\nu s,ir}$ depending on the actual slip s:

$$\omega_{\nu s,ir} = |\omega_s + (\nu_{ir} - 1) \cdot s \cdot \omega_s| \tag{12}$$

These subharmonics cannot be filtered and for the higher harmonics big and bulky filters like in the use of a cycloconverter [7, 8] are necessary. These filters are dispensable when using the M3C with a sufficient high number N of cells.

A low voltage M3C prototype (400V, 15kW) is still in the commissioning process. Each converter arm consists of $N = 5$ cells with a maximum cell capacitor voltage of $u_{c,max} = 160$V and a MOSFET H-bridge. A detailed description of the arm PCBs can be found in [4]. Fig. 4 shows the first experimental results with subconverter one and the resulting voltage waveforms. The subconverter is connected to the 400V, 50Hz grid via a Yz transformer and the line inductors L_e. The load consists of a variable Resistor R_{Load} and is connected between the neutral point of the z-winding arm inductor L and the neutral point of the Yz transformer. The output voltage amplitude is $\hat{U}_r = 300$V, the output frequency is $f_r = 10$Hz and the power transfered to the load $P_r \approx 1.5$kW. The unfiltered line to line input voltage u_{e12} is very close to the desired sinus, only the switching frequency of $f_a = 8$kHz can be seen clearly. The arm voltage u_{11} contains input and output voltage components and the resulting output voltage u_{r1} is sinusoidal due to z-winding arm inductor and transformer working as inductive voltage divider between the three converter arms.

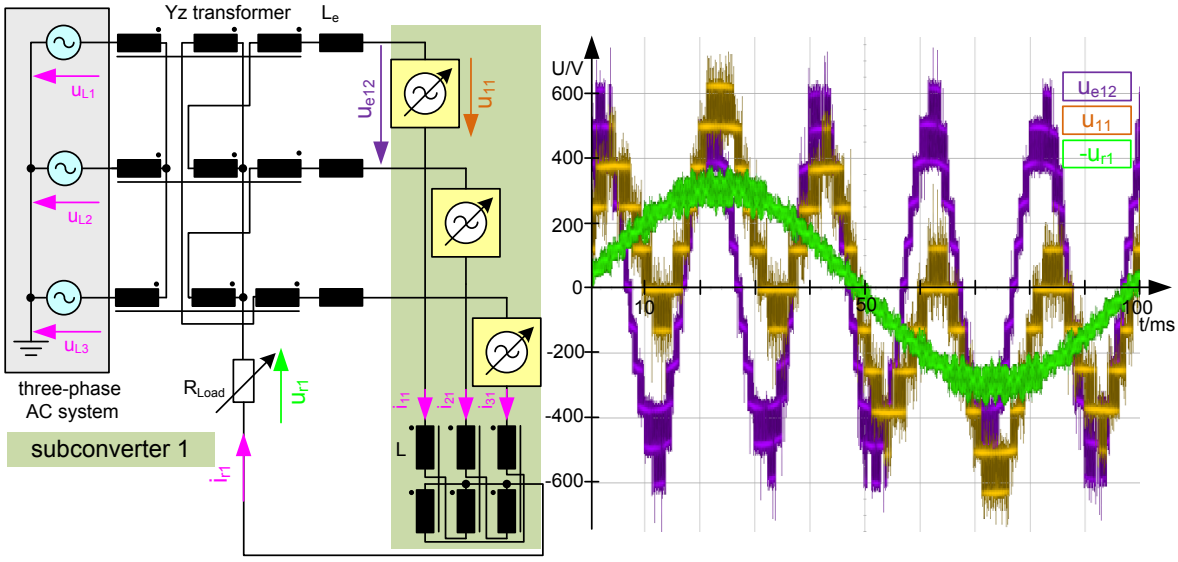

Figure 4: Subconverter test circuit (left) with the measured voltage waveforms (right)

2.5 Operating behavior during grid voltage sags

Grid voltage sags are a big problem for the converters connected to the DFIG because of the generated overvoltages in the rotor circuit which must be handled by crowbars and resistors to protect the converter [7, 8]. During normal operation of the DFIG, the rotor voltage is proportional to the slip (6) and the M3C is dimensioned to handle the maximum rotor voltage $|\underline{U}_{rx,max}|$ at the maximum slip $|s_{max}|$. Without any additional protection the maximum rotor

voltage $|\underline{U}_{rx,sag,max}|$ during a three phase line voltage sag $p \cdot |\underline{U}_{Lx}|$ reaches up to [10, 11]:

$$|\underline{U}_{rx,sag,max}| \approx (1-p)\cdot|s|\cdot k_{DFIG}\cdot|\underline{U}_{Lx}| + p\cdot(1-s)\cdot k_{DFIG}\cdot|\underline{U}_{Lx}| \quad p = \text{relative depth of the sag} \tag{13}$$

$|\underline{U}_{rx,sag,max}|$ decreases with the stator time constant, so after a short time the rotor voltages are below the maximum value during normal operation $|\underline{U}_{rx,max}|$. Fig. 5 shows the behavior for a complete three phase line voltage sag $p = 1$ and a fifty percent line voltage sag $p = 0.5$ for the voltage transfer ratios $k_{DFIG} = 1$ (left) and $k_{DFIG} = 3$ (right). During normal operation, the rotor voltage $|\underline{U}_{rx}|$ corresponds to the red line and changes during the three phase line voltage sag to the green ($p = 0.5$) or purple ($p = 1$) line. The maximum rotor voltage doubles in the over synchronous mode for $k_{DFIG} = 1$ or will be quadrupled for $k_{DFIG} = 3$.

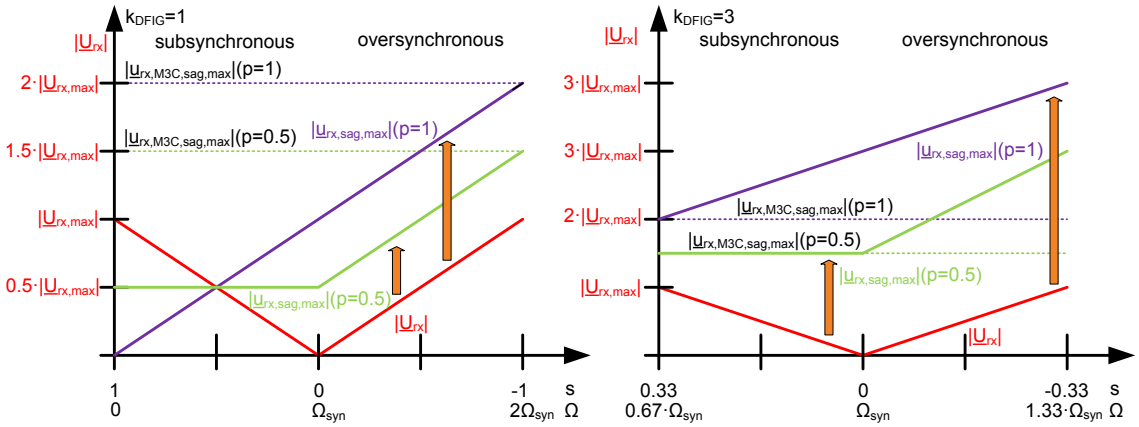

Figure 5: Rotor voltage behavior of the DFIG during 50% ($p = 0.5$) and 100% ($p = 1$) 3 phase line voltage sags for $k_{DFIG} = 1$ (left) and $k_{DFIG} = 3$ (right)

The dotted lines in Fig. 5 show the maximum rotor voltages which can be generated from the M3C for a short time during the sag. They are higher than the maximum rotor voltage $|\underline{U}_{rx,max}|$ during normal operation. This is possible due to the fact, that the minimum arm capacitor voltage (8) is at least the sum of the line and rotor voltage amplitude. This results for $k_{M3C} = 1$ to $u_{cxy,min} \geq 2 \cdot \hat{u}_{rx}$. So the voltage $p \cdot |\underline{U}_{ex}|$ which is not longer needed for the input side can be used immediately to generate temporarily higher rotor voltages to handle the failure and to continue controlling the rotor currents i_{rx}:

$$|\underline{U}_{rx,M3C,sag,max}| = |\underline{U}_{rx,max}| + p \cdot |\underline{U}_{ex}| \tag{14}$$

So, depending on the depth p of the line voltage sag, on the voltage transfer ratio k_{DFIG} and the slip s no crowbar will be necessary. In case that this is not sufficient an oversizing of the M3C resulting in more cells per arm N or a crowbar are possible.

For example, to handle a fifty percent voltage sag without crowbar for $k_{DFIG} = 3$ and $s = -0.33$ a 50% oversizing of the M3C is necessary, resulting in a installed power of $P_{M3C} = 0.33 \cdot P_s \cdot 1.5 = 0.5 \cdot P_s$. Alternatively, using a crowbar with a higher resistance value can be chosen to limit the maximum rotor voltage to $|\underline{U}_{rx,M3C,sag,max}|$ instead of $|\underline{U}_{rx,max}|$. This results in lower rotor currents i_{rx}, less torque peaks to the DFIG and a faster switch back to the M3C after the fault to contine controlling the rotor currents i_{rx}.

The behavior of the M3C together with the DFIG at single phase to ground and phase to phase grid failures [11] needs to be investigated in the future.

3 Conclusion

The Modular Multilevel Matrix Converter (M3C) is presented to feed the rotor circuit of a Doubly Fed Induction Generator (DFIG). The M3C offers several advantages compared to classical solutions like the scalability in the voltage range, which allows higher rotor voltages and lower rotor currents, the scalable redundancy and the multilevel input and output voltages which makes filters dispensable. Additionally, the benefits to generate temporarily higher rotor voltages during a three phase line voltage sag are explained in detail. This may help to have a better control of the rotor currents during the fault.

References

[1] B. Hopfensperger, D.J. Atkinson, and R.A. Lakin. Stator-flux-oriented control of a doubly-fed induction machine with and without position encoder. *Electric Power Applications, IEE Proceedings*, 147(4):241 –250, jul 2000.

[2] A. J. Korn, M. Winkelnkemper, P. Steimer, and J. W. Kolar. *Direct modular multi-level converter for gearless low-speed drives*. Power Electronics and Applications (EPE 2011), Proceedings of the 2011-14th European Conference on, 2011.

[3] F. Kammerer, J. Kolb, and M Braun. A novel cascaded vector control scheme for the Modular Multilevel Matrix Converter. *IECON 2011 Melbourne*, Nov. 2011.

[4] F. Kammerer, J. Kolb, and M. Braun. *Fully decoupled current control and energy balancing of the Modular Multilevel Matrix Converter*. EPE-PEMC 2012 ECCE Europe, Novi Sad, Serbia, 2012.

[5] F. Kammerer, J. Kolb, and M. Braun. *Optimization of the passive components of the Modular Multilevel Matrix Converter for Drive Applications*. PCIM Europe, Nuremberg, Germany, 2012.

[6] W. Kawamura and H. Akagi. Control of the modular multilevel cascade converter based on triple-star bridge-cells (mmcc-tsbc) for motor drives. In *Energy Conversion Congress and Exposition (ECCE), 2012 IEEE*, pages 3506 –3513, sept. 2012.

[7] A. Bocquel and J. Janning. 4* 300 MW Variable Speed Drive for Pump-Storage Plant Application. In *Power Electronics and Applications, 2003 European Conference on*, 2003.

[8] A. Bocquel and J. Janning. Analysis of a 300 MW variable speed drive for pump-storage plant applications. In *Power Electronics and Applications, 2005 European Conference on*, pages 10 pp. –P.10, 0-0 2005.

[9] *PCS 8000 AC Excitation, AC Excitation for hydro pump energy storage plants*. ABB, 2010-07-27.

[10] J. Lopez, P. Sanchis, X. Roboam, and L. Marroyo. Dynamic behavior of the doubly fed induction generator during three-phase voltage dips. *Energy Conversion, IEEE Transactions on*, 22(3):709 –717, sept. 2007.

[11] J. Lopez, E. Gubia, P. Sanchis, X. Roboam, and L. Marroyo. Wind turbines based on doubly fed induction generator under asymmetrical voltage dips. *Energy Conversion, IEEE Transactions on*, 23(1):321 –330, march 2008.